Theoretical Insight into the Spectroscopy and Photochemistry of Isoalloxazine, the Flavin Core Ring

Teresa Climent, Remedios González-Luque, Manuela Merchán, and Luis Serrano-Andrés*

Instituto de Ciencia Molecular, Universitat de València, Apartado 22085, ES-46071 Valencia, Spain

Received: September 5, 2006; In Final Form: October 14, 2006

The electronic singlet−singlet and singlet−triplet electronic transitions of the isoalloxazine ring of the flavin core are studied using second-order perturbation theory within the framework of the CASPT2//CASSCF protocol. The main features of the absorption spectrum are computed at 3.09, 4.28, 4.69, 5.00, and 5.37 eV. The lowest singlet (S_1) and triplet (T_1) excited states are found to be both of π character with a singlet−triplet splitting of 0.57 eV. On the basis of the analysis of the computed spin−orbit couplings and the potential energy hypersurfaces built for the relevant excited states, the intrinsic mechanism for photoinduced population of T_1 is discussed. Upon light absorption, evolution of the lowest singlet excited state along the relaxation pathway leads ultimately to the population of the lowest triplet state, which is mediated by a singlet−triplet crossing with a state of nπ* type. Subsequently a radiationless decay toward T_1 through a conical intersection takes place. The intersystem crossing mechanism and the internal conversion processes documented here provide a plausible route to access the lowest triplet state, which has a key role in the photochemistry of the flavin core ring and is mainly responsible for the reactivity of the system.

1. Introduction

Substances that contain the *isoalloxazine* ring are called *flavins* and the flavin-containing proteins are known as *flavoproteins*.[1] Phototropin is a plasma membrane associated protein that constitutes a relevant and well-known example of flavoprotein and regulates phototropism response of higher plants by using two isoforms (phot1 and phot2), as well as chloroplast photorelocation, and cell stomatal opening.[2,3] Phototropin acts as a blue-light sensitive photoreceptor having two LOV (light, oxygen, and voltage) domains, LOV1 and LOV2, and uses as chromophore a noncovalently bound single flavin mononucleotide (FMN) (see Figure 1) per domain.[4]

It is accepted among the scientific community that the primary step of the FMN photocycle after light absorption involves population of the lowest singlet excited state (S_1) and subsequently a rapid decay to the lowest triplet excited state (T_1) takes place through an intersystem crossing (ISC) mechanism.[5,6,7,8,9] The fate of the photoinduced electron transfer to triplet flavins, which behave like acceptors, has been indeed extensively analyzed by using different experimental techniques.[10,11] Nevertheless, a detailed account for the singlet−triplet nonradiative process within the framework of nonadiabatic photochemistry has not been yet provided. In particular, the key issue seems to be whether relaxation to the triplet state involves a direct coupling between the lowest singlet and triplet states or proceeds via a third excited state. Surprisingly, despite the relevance of flavoproteins, just a few theoretical studies on the excited states of related systems have been previously carried out, either by employing density functional theory (DFT) schemes or by using semiempirical methodologies.[6,12−14] To the best of our knowledge, there are no high-level ab initio studies offering a detailed mechanism on the photochemistry of isoalloxazine (benzo[*g*]pteridine-2,4(3*H*,10*H*)-dione), the flavin core ring. Analysis of the photochemical behavior of the isoalloxazine ring on the basis of accurate (predictive) quantum-chemical computations has been the underlying reason to undertake the present research. As a first step toward the understanding of the isoalloxazine photochemistry on theoretical grounds, the main vertical and adiabatic electronic transitions of the molecule are initially considered. The electronic spectra of lumiflavin, 8-methylisoalloxazine, and riboflavin show the same characteristics and can be described as typical of isoalloxazines.[15] In the energy region up to 5.5 eV, the absorption spectra of these systems are composed mainly of three bands. On the other hand, no significant differences have been found in the polarization spectra of lumiflavin, riboflavin, and FMN with respect the parent molecule, the oxidized form of the isoalloxazine ring,[16] which can therefore be expected to be responsible for the flavin photochemistry.

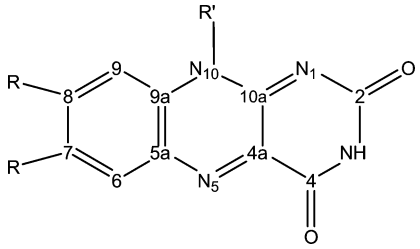

Figure 1. Structure and labeling of the isoalloxacine ring and related flavins.

We report here comprehensive theoretical research on the valence excited states of the isoalloxazine molecule making possible confident assignments. Furthermore, the results provided can serve as calibration for less computationally demanding methods. The excited states of the system have been characterized by using multiconfigurational second-order perturbation theory through the CASPT2 method.[17] The successful performance of the CASPT2 approach in the interpretation of the electronic spectra of a large number of organic compounds

* To whom correspondence should be addressed. E-mail: Luis.Serrano@uv.es.

10.1021/jp065772h CCC: $33.50
Published on Web 11/22/2006

is well established.[18−26] Particularly related to the present work are the previous studies performed on chromophores of different biomolecules, such as the protonated Schiff base of retinal (PSB),[27] the chromophore of the Photoactive Yellow Protein (PYP),[28] and the DNA nucleobases cytosine[29] and adenine.[30] The present work includes determination of vertical transition energies, band origins, and emission maxima related to the low-lying valence singlet and triplet excited states. In addition, on the basis of the analysis performed for the relaxation pathway along the S_1 hypersurface, it is concluded that the coupling between $S_1(\pi\pi^*)$ and $T_1(\pi\pi^*)$ does not occur directly but is mediated by a high-lying electronic triplet state, $^3(n_{N-}\pi^*)$, which involves the one-electron promotion from the minus linear combination of the lone-pair molecular orbitals (MOs), implying the nitrogen atoms, to the π system.

Computational details are described in the following section. Next, the equilibrium geometry computed for the ground and low-lying excited states, as well as the CASPT2 vertical and adiabatic singlet → singlet and singlet → triplet absorption spectra, together with other spectroscopic features, are presented and discussed. Finally, the current picture on the photochemistry of isoalloxazine obtained from global research is addressed. Our conclusions are summarized in the last section.

2. Computational Details

Geometry optimization of the ground and low-lying valence excited states were carried out at the CASSCF level.[31] The π-valence active space of the isoalloxazine ring involves 18 electrons and 16 molecular orbitals (MOs), hereafter denoted by CASSCF(18,16). For the computation of the excited states of $\pi\pi^*$ character, and after careful calibration calculations, it could be decreased to 14 π-valence electrons distributed among 13 π-valence MOs, resulting in the CASSCF(14,13) wave function. In order to study the $n\pi^*$ states, the active space was enlarged with the corresponding lone-pair MOs, keeping inactive the π MO with the highest occupation number in the preceding CASSCF(14,13) treatment and considering as secondary the π MO with the lowest occupation number, finally yielding the CASSCF(16,13) wave function. It is a reasonable choice that largely fulfills the required flexibility to describe the $n\pi^*$ states. The basis set 6-31G(d) was used throughout. Inclusion of polarization functions on the hydrogen atoms by using the 6-31G(dp) basis set had a minor effect on the computed electronic transition energies.

Exploratory calculations in different regions of the hypersurfaces starting from well distorted geometries led to basically planar singular points in all the cases for ground and excited states; therefore, according to our research, the molecule keeps planarity during the photochemical reaction. The vertical transition energies were then computed within the constraints of C_s symmetry, making the computation more technically tractable. The MOs for the vertical excited states were obtained from average CASSCF computations, where the averaging includes all states of interest within a given symmetry: eight roots for $^1A'$ states, two roots for $^{1,3}A''$ states involving the lone-pair MOs (treating those located on the oxygen or nitrogen atoms in separate calculations but using the same scheme for the active space), and one root for the lowest $^3A'$ state. To take into account the remaining electron correlation effects, the CASSCF wave functions were employed as reference in a single-state second-order perturbation CASPT2 treatment.[17] In addition, the effect of weakly interacting intruder states was minimized by using the so-called imaginary level-shift technique.[32] After the usual calibration, a shift of 0.3 au was selected to compile the final results. The vertical energy of each excited stated is referred to the ground-state energy computed with the same active space. The carbon, nitrogen, and oxygen 1s electrons were kept frozen in the form determined by the ground-state closed-shell Hartree−Fock wave function and were not correlated at the second-order level.

The CASSCF state interaction (CASSI) method[33,34] was used to calculate the transition dipole moments (TDMs) from the CASSCF wave functions. The corresponding CASSCF TDM and the energy difference obtained in the CASPT2 computation were used in the formula for the oscillator strength, and similarly to estimate the radiative lifetimes by using the Strickler−Berg relationship.[35,36]

From the Franck−Condon (FC) geometry, a minimum energy path (MEP) for the lowest singlet excited electronic state (S_1) of the system was computed by using a new recently developed algorithm for constrained optimizations.[37] The evolution of the states was mapped by computing at each MEP coordinate the CASPT2 energies, for both the singlet and triplet excited states of interest. The spin−orbit coupling (SOC) has been estimated as described in detail in a related study on the triplet-state formation along the ultrafast decay of excited cytosine.[38] All computations in the present paper use the MOLCAS 6.0 quantum chemistry package.[39,40]

3. Results and Discussion

As a preliminary step toward the theoretical understanding of the electronic spectra of isoalloxazine, the optimized geometries computed for the ground state and the low-lying singlet and triplet excited states of the molecular model considered are first presented. The properties of the excited states calculated vertically are next analyzed. After that, the nonvertical transition energies are discussed. Finally, the photoinduced population of the lowest triplet state along the relaxation path of S_1 is addressed. The present findings will be compared with the available experimental data and previous theoretical findings.

3.1. Equilibrium Structures. The CASSCF optimized geometric parameters for the ground state $(gs)_{min}$ and the lowest singlet and triplet excited states of $\pi\pi^*$ character, $^1(\pi\pi^*)_{min}$ and $^3(\pi\pi^*)_{min}$, respectively, are depicted in Figure 2. In addition, the results for the triplet state $^3(n_{N-}\pi^*)$, particularly relevant for the rationalization of photochemical behavior of the molecule, are also included. The Cartesian coordinates for the optimized structures can be found in the Supporting Information.

Most of the computed bond distances for the ground state deviate by less than 0.020 Å from the available crystallographic data.[41] Since isoalloxazine tautomerizes immediately to alloxazine by a N_{10} to N_1 proton shift, the simplest suitable derivative to compare with corresponds to 10-methylisoalloxazine.[41] The agreement between the CASSCF results obtained for the ground state and the X-ray data is satisfactory. Therefore, it can be inferred that the methyl substituent plays a minor role in determining the equilibrium structure of the fused-ring molecular system. A similar situation is expected for the spectroscopic properties.

The major geometric changes taking place for the $^1(\pi\pi^*)_{min}$ and $^3(\pi\pi^*)_{min}$ structures, with respect to the ground state $(gs)_{min}$, involve an increase of the N_1-C_{10a} and $C_{4a}-N_5$ bond distances and of the $C_{5a}-C_{9a}$ bond length to a lesser extent, whereas a decrease of the $C_{4a}-C_{10a}$ bond distance is also noted. In terms of the natural orbitals (NOs) of the CASSCF wave function, the excited states $^1(\pi\pi^*)$ and $^3(\pi\pi^*)$ are described mainly by a one-electron promotion from the NO topologically equivalent to the highest occupied MO (HOMO-like) to the lowest

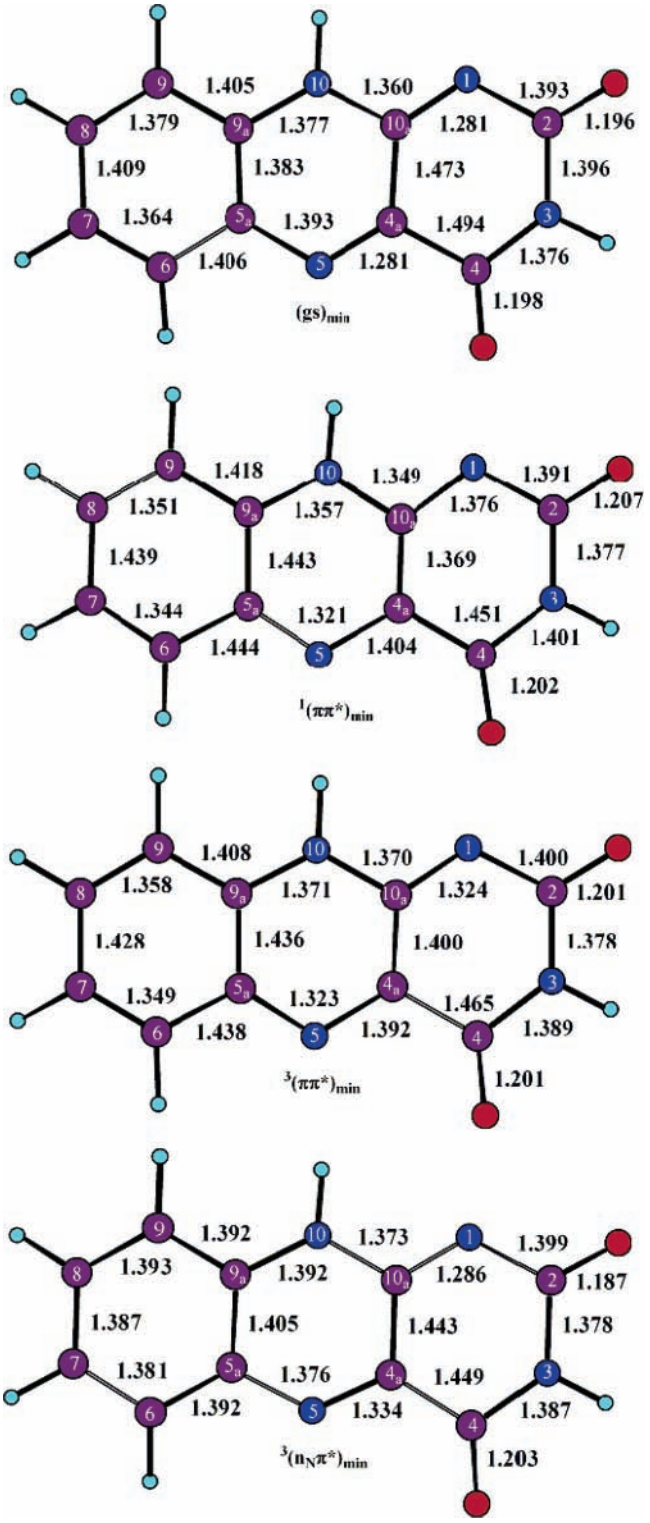

Figure 2. Optimized CASSCF/6-31G(d) structures for the ground and low-lying excited states.

unoccupied MO (LUMO-like). Therefore, the pattern found for the variations in geometry upon excitation correlates nicely to the relative electron-density shifts concomitant to the HOMO/LUMO-like electron redistribution. As can be seen in the Supporting Information, in the HOMO-like NO the electron density is mainly localized in the nitrogen atom N_1 and in the $C_{5a}-C_{9a}$ bonding region. For the LUMO-like NO, the electron density increases considerably in the region of the $C_{4a}-C_{10a}$ bond and the nitrogen atom N_5. The occurrence of the reported geometric changes can be seen just as the response of the electronically excited molecule to such electron reorganization. Similarly, the geometry computed for the $^3(n_{N-}\pi^*)$ state is consistent with migration of electron density from the lone pairs located on the nitrogen atoms to the π system, basically toward the LUMO-like NO.

The optimized geometries were employed to characterize the vertical electronic spectra (absorption and emission) and nonvertical electronic transitions.

3.2. Vertical Spectra. The computed vertical excitation energies at the CASSCF and CASPT2 levels of theory, together with oscillator strengths of the related electronic transitions, dipole moments for the states, and selected experimental data are listed in Table 1. The resulting assignments for the excited states are given within parentheses in the first column of Table 1, identifying the different excited states obtained for the isoalloxazine ring, where n_{N-} and n_{N+} represent the minus and plus linear combinations of the in-plane lone pairs belonging to the N_1 and N_5 atoms (see Figure 1 for atom labeling). The same applies for the two oxygen atoms: n_{O-} and n_{O+}. For the sake of brevity, the lowest singlet $2^1A'(\pi\rightarrow\pi^*)$ and triplet $1^3A'(\pi\rightarrow\pi^*)$ excited states will be hereafter called S_1 and T_1, respectively, and the $1^3A''(n_{N-}\rightarrow\pi^*)$ state will be denoted by T_N. As discussed below, this state might be especially involved in the deactivation of the S_1 state and subsequent population of the lowest triplet T_1 state.

At the highest level of theory employed, five valence electronic transitions involving excited states of $\pi\pi^*$ character are computed with significant oscillator strength and can be related to the main features of the recorded electronic spectrum up to 5.5 eV. Only one transition is found in the visible range at 3.09 eV, corresponding to the vertical absorption from the ground state (S_0) to the lowest singlet excited state. The $S_0 \rightarrow S_1$ transition has an associated oscillator strength of about 0.2. As stated above, in terms of the NOs of the CASSCF wave function, S_1 involves electron reorganization from the HOMO-like to the LUMO-like NOs. As the S_1 dipole moment (9.7 D) is much larger than that of the ground state (2.4 D), the occurrence of a red shift in polar solvents can be expected for the lowest energy transition. This is consistent with the absorption spectra reported by Sun et al.[15] for methylisoalloxazine derivatives in ethanol at 77 K, where a maximum peaking at 2.85 eV is observed for 8-methylisoalloxazine and at 2.76 eV for lumiflavin, 3-methyllumiflavin, and riboflavin. The lowest singlet excited state of $n\pi^*$ type (T_N) is calculated to lie vertically at 3.34 eV, that is, close to the lowest transition. As expected, the intensity of the transition is predicted to be exceedingly weak (oscillator strength 0.007). Nevertheless, because of the close proximity of the $n\pi^*$ and $\pi\pi^*$ states, they could further interact by vibronic coupling and the resulting feature could be related to the shoulder observed in the high region of the lowest energy visible band recorded in ethanol.[15]

The second energy band recorded experimentally can be related to the electronic transition $1^1A' \rightarrow 3^1A'$ of $\pi\pi^*$ nature computed in vacuo at 4.28 eV and with a slightly smaller oscillator strength than that obtained for the lowest transition. The vertical result is somewhat blue shifted with respect to the corresponding band maximum observed at 3.62−3.76 eV in solution (depending on the methyl derivative).[15] Absorption and fluorescence studies[42] made on different isoalloxazines have concluded that an increase of the solvent polarity has only a little influence on the lowest energy absorption maximum, whereas the maximum in the second energy band exhibits a pronounced bathochromic shift. Accordingly, the dipole moment calculated for the $3^1A'$ state is indeed larger than that for the

TABLE 1: Experimental and Computed CASSCF And CASPT2 Excitation Energies, Related Oscillator Strengths (*f*), and CASSCF Dipole Moments (μ) for the Vertical Excited States of Isoalloxazine

	excitation energy (eV)				
state[a]	CASSCF	CASPT2	*f*	μ (D)	experimental[b]
ground state					
$1^1A'$				2.4	
singlet excited states					
$2^1A'(\pi\rightarrow\pi^*)$	4.15	3.09	0.239	9.7	2.85
$1^1A''(n_{N-}\rightarrow\pi^*)$	4.79	3.34	0.007	5.4	
$2^1A''(n_{O-}\rightarrow\pi^*)$	5.15	3.75	0.001	1.9	
$3^1A'(\pi\rightarrow\pi^*)$	5.47	4.28	0.158	10.1	3.76
$3^1A''(n_{O+}\rightarrow\pi^*)$	5.62	4.43	0.000	2.6	
$4^1A''(n_{N+}\rightarrow\pi^*)$	5.83	4.66	0.001	5.0	
$4^1A'(\pi\rightarrow\pi^*)$	6.27	4.69	0.104	7.8	
$5^1A'(\pi\rightarrow\pi^*)$	5.88	4.90	0.035	7.9	
$6^1A'(\pi\rightarrow\pi^*)$	6.78	4.92	0.058	1.8	
$7^1A'(\pi\rightarrow\pi^*)$	7.16	5.00	0.337	7.1	4.68−4.77
$8^1A'(\pi\rightarrow\pi^*)$	7.48	5.37	0.641	5.5	
triplet excited states					
$1^3A'(\pi\rightarrow\pi^*)$	3.14	2.52		6.0	
$1^3A''(n_{N-}\rightarrow\pi^*)$	4.30	2.97		6.3	
$2^3A''(n_{O-}\rightarrow\pi^*)$	4.99	3.70		2.2	
$3^3A''(n_{O+}\rightarrow\pi^*)$	5.47	4.39		2.8	
$4^3A''(n_{N+}\rightarrow\pi^*)$	5.57	4.53		5.1	

[a] The character and ordering of the states are those obtained with the CASPT2 method. [b] Band maxima (eV) from the absorption spectrum of 8-methylisoalloxazine in ethanol at 77 K.[15]

$2^1A'$ state and consequently a larger red shift should occur in polar solvents for the second energy band maximum. Since two $n\pi^*$ states involving the lone pairs of the carbonyl group are energetically close, an interaction with the $2^1A'(\pi\rightarrow\pi^*)$ state may also occur, leading to a complex band envelope where the maximum might not necessarily be coincident with the vertical feature here computed, which is more a rule than an exception as far as the spectroscopy of the carbonyl group is concerned.[24] Because of the large difference between the ground and excited state geometries, the spectroscopic features related to CO bonds are characterized by long vibrational progressions, and as a result the maximum of the band does not match the vertical transition, as is commonly assumed within the FC principle.[22,43] Taking into account the error bars of the computation (0.1−0.2 eV), the absence of the methyl group in the calculation, and the possible solvent influence, one could easily conclude that the agreement between theory and experiment can be regarded as satisfactory. Nevertheless, experience has shown us that when the deviation of vertical CASPT2 result from the observed maximum is significant, as much as 1/2 eV as is the case here, it points to the nonvertical nature of the recorded band. This issue could only be resolved by carrying out computationally a vibrational resolution of the band, a formidable task at present for a system of the molecular size of isoalloxazine, but that might hopefully be undertaken soon with the expected advances to be seen from both software and hardware standpoints.

The third energy band of isoalloxazines in ethanol solution has a band maximum in the 4.7−4.8 eV energy range.[15] From 4.7 to 5.4 eV five electronic transitions are computed that might contribute to the observed spectra. Most of the states have dipole moments higher than the ground state, and consequently the computed transitions are expected to be somewhat blue shifted with respect to the recorded data in ethanol, a constant behavior found in the present system for the transitions bearing the largest oscillator strengths. Thus, we conclude that the third energy band is the result of several $\pi\pi^*$ electronic transitions, in particular those taking place from the ground state to the $4^1A'$ (4.69 eV), $7^1A'$ (5.00 eV), and $8^1A'$ (5.37 eV) excited states, which have significant oscillator strengths (cf. Table 1) and therefore constitute the main contributors to the band. The

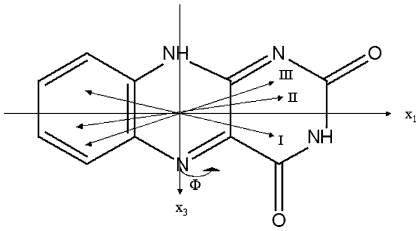

Figure 3. Polarization directions for the low-energy electronic transitions (I, II, and III) in the absorption spectrum of isoalloxazine. Using a previous criterion,[16] the angle Φ has been calculated with respect to the x_3 short axis.

CASSCF wave functions of the $4^1A'$ and $7^1A'$ excited states have a dominant participation of the singly excited HOMO → LUMO+1 configuration. The two $\pi\pi^*$ states $5^1A'$ and $6^1A'$ can be described mainly as the result of the HOMO−2 → LUMO one-electron configuration with contributions of the two-electron promotions from the HOMO to the LUMO in the former and the HOMO−3 → LUMO in the latter.

As can be seen in Table 1, a number of $n\pi^*$ states are interleaved among the main valence transitions. The $1^1A''(n_{N-}\rightarrow\pi^*)$, $2^1A''(n_{O-}\rightarrow\pi^*)$, $3^1A''(n_{O+}\rightarrow\pi^*)$, and $4^1A''(n_{N+}\rightarrow\pi^*)$ states are placed vertically at 3.34, 3.75, 4.43, and 4.66 eV, respectively. The computed oscillator strengths associated with those transitions are negligible and therefore do not have special relevance with regard to the absorption spectrum.

Further support for the proposed assignments can be obtained by analyzing the polarization directions computed for the main transitions, which are depicted in Figure 3, with respect to the available experimental data.

The results $\Phi_I = 75°$, $\Phi_{II} = 100°$, and $\Phi_{III} = 120°$, where Φ_I, Φ_{II}, and Φ_{III} are the angles of the transition dipole moment of each band with respect to the short molecular axis, are consistent with those determined experimentally.[15,16,44] In particular, the relative angle between the computed TDM obtained between the lowest and second energy bands is close to that deduced by Sun et al.,[15] $\Phi_{I,II} = 20° \pm 5°$, from fluorescence polarization data. As compared to the data reported by Johansson et al.,[16] $\Phi_I = 58° \pm 4°$, $\Phi_{II} = 97° \pm 3°$, and $\Phi_{III} = 119° \pm 2°$, a large deviation for Φ_I is noted, although both

TABLE 2: Computed Vertical Transition, Band Origin, and Vertical Emission Energies and Radiative Lifetimes (τ_{rad}) for the Low-Lying Singlet Excited States of Isoalloxazine

	vertical transition (eV)		band origin (eV)		vertical emission (eV)		
state	CASSCF	CASPT2	CASSCF	CASPT2	CASSCF	CASPT2	τ_{rad}
singlet states							
$\pi\pi^*$	4.15	3.09	3.20	2.69	2.21	2.04	15 ns
$n_N\pi^*$	4.79	3.34	3.82	3.33	2.65	2.61	467 ns
$n_O\pi^*$	5.15	3.75	3.52	3.16	2.19	2.33	6458 ns
triplet states							
$\pi\pi^*$	3.14	2.52	2.41	2.03	1.73	1.75	116 ms
$n_N\pi^*$	4.30	2.97	3.50	2.73	3.00	2.37	
$n_O\pi^*$	4.99	3.70	3.40	3.10	2.20	2.34	

theory and experiment agree in the long-axis polarization character of the band. It is worth mentioning, however, that the theoretical prediction matches the value given by Eaton et al.[44] ($\Phi_I = 75°$). The present results would hopefully help to elucidate the discrepancy between the mentioned sets of experimental data.[16,44]

The ordering and nature of the five lowest valence triplet states is the same as that obtained for the singlet excited states. The singlet−triplet spectrum computed at the ground-state geometry of isoalloxazine places the lowest triplet state $1^3A'(\pi\rightarrow\pi^*)$ at 2.52 eV. Next, at 2.97 eV, the $1^3A''(n_{N-}\rightarrow\pi^*)$ state is located. As can be seen in Table 1, the remaining $n\pi^*$ triplet states are found within the energy range 3.70−4.53 eV. As expected, the largest singlet−triplet splitting is computed for the low-lying $\pi\pi^*$ states (0.57 eV). Assuming that both singlet and triplet states are described by the same MOs, in a simple molecular orbital model the exchange integral is related to the singlet−triplet energy difference. Normally, since that integral is relatively larger for $\pi\pi^*$ than for $\sigma\pi^*$ states, the singlet−triplet splitting becomes more pronounced in states of $\pi\pi^*$ character. Thus, except for the pair $^{1,3}A''(n_{N-}\rightarrow\pi^*)$, which has a singlet−triplet energy difference of 0.37 eV, the other singlet−triplet gaps are at most 0.1 eV. Since the states discussed are described mainly by singly excited configurations, that elementary reasoning holds true despite the use of large and complex CASSCF wave functions.

As far as we are aware, no theoretical studies have been performed on the excited states of isoalloxazine itself. However, time-dependent DFT results on related compounds have offered a similar three-band view of the singlet−singlet spectrum attributed to ($\pi\rightarrow\pi^*$) transitions,[6] whereas the relative placement of the lowest ($n\rightarrow\pi^*$) transition seems to depend on the details of the computational procedure.[6,11]

3.3. Emission and Nonvertical Transition Energies. Knowledge of the energy hypersurfaces of the ground and low-lying excited states of isoalloxazine is essential for the determination of spectroscopic properties, which are particularly relevant in an ample group of biologically active chromophores. The basic understanding of the spectroscopic behavior of these compounds requires not only the accurate computation of the vertical states but also the characterization of the emission and nonvertical transition energies.

The computed transitions involve the energy difference between the ground state and the excited state at the respective optimized geometries and the vertical emission from the excited-state minimum vertically to the ground state. The lowest component of each absorption band is the 0−0 absorption, also labeled T_0, and involves the lowest vibrational states. The value computed here is, however, T_e, obtained as the difference of the adiabatic electronic energy values. On the other hand, the computed vertical emission (fluorescence or phosphorescence) can be considered as a lower bound for the observed maximum of the emission band. Since the active spaces are the same as those employed in the geometry optimizations and for the computation of vertical transitions (a π-valence plus lone-pairs MO as appropriate), a consistent comparison can be then performed between the computed absorption and emission spectra. The study includes determination of both vertical and adiabatic transitions related to absorption and emission bands for the three lowest valence excited $\pi\pi^*$ and $n\pi^*$ states in the singlet and triplet manifolds as listed in Table 2.

For the lowest singlet−singlet feature ($\pi\pi^*$ type), the vertical and the adiabatic transitions are computed within 0.4 eV, with a fluorescence band origin predicted at 2.69 eV and a vertical emission at 2.04 eV. The obtained results can be directly related to the reported spectra of 8-methylisoalloxazine in ethanol,[15] displaying low-lying absorption and emission band origins near 2.7 eV and fluorescence band maxima between 2.5 and 2.3 eV. The computed radiative lifetime, 15 ns, is also in agreement with the experimental datum for the fluorescence lifetime of the methylisoalloxazine derivates (15.1 ns for 3,10-dimethylisoalloxazine in acetonitrile solution[42]).

On the basis of relatively long lifetimes and the tendency for negative phosphorescence polarization in the 0−0 region with respect to the lowest $\pi\pi^*$ transitions, the phosphorescent triplet state of isoalloxazines has been assigned as a $^3(\pi,\pi^*)$ type.[15] Our computed results are in agreement with that suggestion, predicting that the lowest triplet state has (π,π^*) character with the phosphorescence band origin at 2.03 eV and vertical emission at 1.75 eV, in relatively good agreement with the reported values for 8-methylisoalloxazine in ethanol,[15] near 2.2 and 2.0 eV, respectively. A detailed account for the intrinsic mechanism of the T_1 population is subsequently considered.

3.4. Triplet-State Formation. Upon near-UV light irradiation, the isoalloxazine system is expected to be promoted to the lowest excited state of the same symmetry as the ground state (singlet). As presented above, the vertical transition to S_1 at the FC geometry was computed to be 3.09 eV with an oscillator strength of around 0.2. To analyze the evolution of S_1, once that the initial absorption took place, a minimum energy path (MEP) along the S_1 reaction coordinate was computed at the CASSCF level. At the stationary geometries so obtained along the path, a number of singlet and triplet excited states were subsequently calculated at the CASPT2 level (see Supporting Information), yielding in this manner a static picture of the energetic variations that suffer the different states along the S_1 MEP. A representation of the main photochemical processes occurring is schematically shown in Figure 4.

Along the relaxation pathway on S_1, the first event is the occurrence of a near degeneracy between S_1 and T_N, close in the FC region, leading to a singlet−triplet crossing denoted by $(S_1/T_N)_{STC}$. In the vicinity of such a crossing the ISC mechanism is favorable in the two required aspects, i.e., the close energetic proximity of both states and the relatively large SOCs. As can

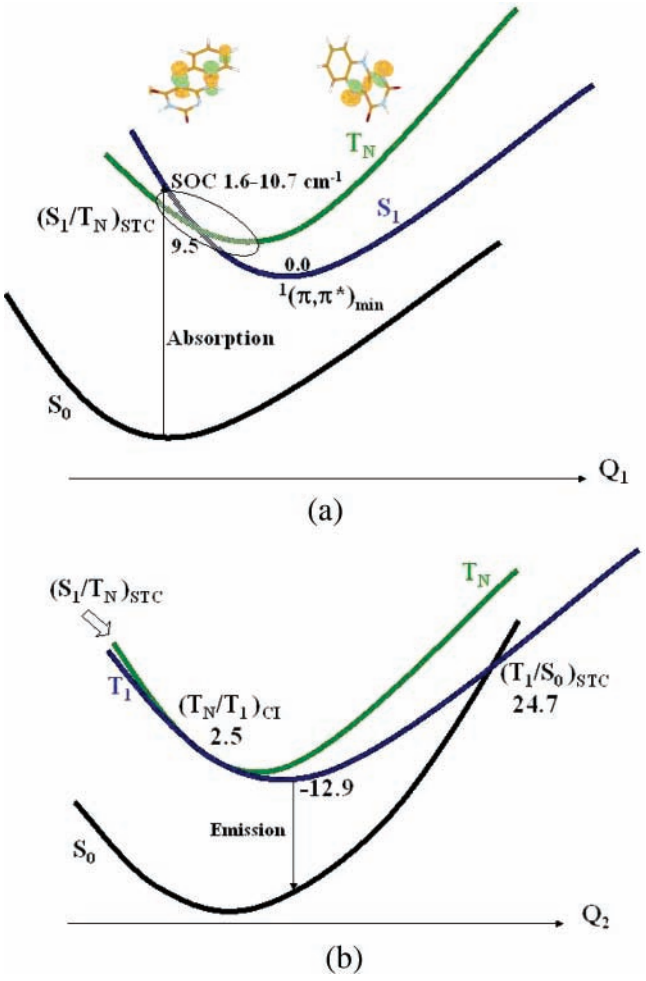

Figure 4. Schematic representation of the photochemical events after light absorption once isoalloxazine has been promoted vertically to S_1. (a) Population of T_N in the vicinity of Franck−Condon region by intersystem crossing mechanism. (b) Internal conversion toward T_1 mediated by the $(T_N/T_1)_{CI}$ leading ultimately to the $^3(\pi\pi^*)_{min}$ structure. Energies are in kcal·mol^{-1}. Q_1 and Q_2 are reaction coordinates.

be seen in Figure 4a, the computed electronic SOC around this region ranges from 2 to 11 cm^{-1}, reflecting the spin−orbit allowed character of the $^1(\pi,\pi^*)/^3(n,\pi^*)$ transition as enunciated by the El-Sayed selection rules for intersystem crossing.[45] Further along the path the equilibrium structure of the lowest singlet excited state, $^1(\pi,\pi^*)_{min}$, is ultimately reached. It is worth mentioning that T_1 is placed below S_1 all the way along the S_1 relaxation path. Thus, one can envisage that upon absorption of a photon, the isoalloxazine ring is promoted to its lowest singlet excited state, S_1, which partially decays in times shorter than the experimental time resolution to an intermediate related to T_N. The population transfer occurs before the S_1 minimum is encountered, which is consistent with the fact that the fluorescence quantum yields of the flavin compounds are lower than the intersystem crossing quantum yield and triplet state formation.[46] Polar solvents seem to increase ISC and decrease fluorescence quantum yields in isoalloxazines.[15,42] According to their nature, $S_1(\pi\pi^*)$ and $T_N(n\pi^*)$ would be in polar media stabilized and destabilized, respectively, with respect to the in vacuo values, leading to a decrease in the vertical energy gap and a singlet−triplet crossing, which might occur closer to the FC region, favoring the trends observed experimentally.

As an inset of Figure 4a, the structures of isoalloxazine showing the π and N_5 lone-pair orbitals involved in the spin flip are shown. A comparative analysis of the Mulliken population per center at the geometries around the FC zone, with respect to the $^1(\pi,\pi^*)_{min}$ and $^3(n_N,\pi^*)_{min}$ structures, allows us to conclude that N_5 is the center directly implied in the spin flip. The fact that the carbon atom C_{4a} has a minor relevance in this issue is somewhat counterintuitive since the molecule distortion in the T_N state with respect to S_1 occurs in the axis involving the $N_1-C_{10a}-C_{4a}-N_5$ atoms and comprises the shortening of the N_1-C_{10a} and $C_{4a}-N_5$ bond distances, as well as an increase of the $C_{10a}-C_{4a}$ bond length.

Starting from $(S_1/T_N)_{STC}$, evolution of the $^3(n_N,\pi^*)$ state has been studied by following a similar computational strategy. The CASSCF MEP along the $^3(n_N,\pi^*)$ state was first calculated and, at the corresponding T_N-MEP coordinates, the singlet and triplet states were computed at the CASPT2 level. The results from this part of the research are summarized in Figure 4b. Once T_N is populated, a rapid T_N to T_1 internal conversion takes place, mediated by the $(T_N/T_1)_{CI}$ conical intersection, which is computed to be at 2.5 kcal/mol (0.11 eV) above the $^1(\pi,\pi^*)_{min}$, the reference structure chosen for the relative energies depicted in Figure 4. The T_N MEP leads ultimately to the equilibrium structure of the T_1 state, $^3(\pi,\pi^*)_{min}$, placed 12.9 kcal/mol (0.56 eV) below $^1(\pi,\pi^*)_{min}$. From relaxed T_1, three different photochemical events could take place: emission (phosphorescence), reactivity of the long-lived T_1 isoalloxazine with different protein residues, and radiationless decay to the ground state through a $(T_1/S_0)_{STC}$. In order to explore the latter possibility, the $(T_1/S_0)_{STC}$ structure was actually computed. With the system located initially at the $^3(\pi,\pi^*)_{min}$ point of the hypersurface, the energy barrier to overcome in order to access the $(T_1/S_0)_{STC}$ is 37.6 kcal/mol at the CASPT2 level. Therefore, to deactivate T_1 isoalloxazine to the ground state nonradiatively via the $(T_1/S_0)_{STC}$ crossing ultimately depends on the excess of vibrational energy in the system at this point; otherwise the molecule will just emit. As compiled in Table 2, the radiative lifetime for T_1 is on the order of 116 ms, consistent with the nature of the state. On the other hand, it is known that, after T_1 formation, the flavin core ring, the chromophore of phototropin, reacts with the sulfur atom of the cysteine-39 to form an adduct. To get further insight into that process, and as a natural continuation of the present study, an ongoing project is addressed toward modeling the reactivity of isoalloxazine in T_1 with sulfur-containing compounds.

4. Summary and Conclusions

The electronic excited states of isoalloxazine were studied using high-level ab initio quantum-chemical methods based on multiconfigurational wave functions. In particular, the CASPT2 multiconfigurational second-order perturbation theory, in conjunction with equilibrium geometries determined at the CASSCF level, i.e., the CASPT2//CASSCF protocol, was employed. The vertical excitation energies were computed at the CASPT2 level using the CASSCF optimized geometry for the ground state. The study comprised excited states in the singlet manifold up to 5.5 eV. Eleven singlet and five triplet vertical excited states were characterized. The overall picture of the obtained spectra as regards the nature of the states, polarization directions of the transitions, and relative intensities of the main absorption bands shows satisfactory agreement with the available experimental data. The main vertical features of the absorption spectrum computed in vacuo at 3.09, 4.28, 4.69, 5.00, and 5.37 eV are, however, somewhat blue shifted with respect to the experimental data in solution. To estimate the band origin and emission maximum, geometry optimizations for the lowest singlet and triplet excited states were also carried at the CASSCF level. The lowest vertical singlet−singlet (at 3.09 eV) and

singlet−triplet (at 2.52 eV) transitions are of $\pi\pi^*$ character. The corresponding band origins are placed at 2.69 and 2.03 eV, respectively. We have analyzed in detail the possibility of populating the lowest triplet state of isoalloxazine along the relaxation path of the lowest singlet state. For this purpose, spin−orbit couplings and potential energy hypersurfaces for the relevant excited states were computed. The theoretical analysis reveals that the intrinsic mechanism for photoinduced population of T_1 has two steps. First, in a wide region close to the vertical transition of S_1, a singlet−triplet crossing by an intersystem crossing mechanism involving a triplet state of $n\pi^*$ type is favored. Second, from this point of the hypersurface, further along the relaxation pathway of the triplet $n\pi^*$ state, a conical intersection implying the two lowest triplet states is found, leading directly to relaxed T_1, mainly responsible for the inherent reactivity of the flavin core ring.

We can finally conclude that triplet-state formation, responsible for triggering the photochemical cycle of flavin-related compounds, is revealed from the present results in vacuo as an intrinsic property of the isoalloxazine molecule. Although the protein environment does indeed increase the intersystem crossing rate[46] and is clearly necessary for adduct formation, the chromophore itself becomes the main actor in the initial part of the photocycle, showing an implicit ability to populate efficiently the lowest triplet state, a property that has been most probably evolved as the optimal biochemical-function response of flavoproteins to sunlight and environmental exposure.

Acknowledgment. The research reported has been supported by the Spanish MEC-FEDER, Project No. CTQ2004-01739, and the Generalitat Valenciana, Project No. GV06-192.

Supporting Information Available: Cartesian coordinates of the most relevant structures employed, calculated CASPT2 MEPs along the $S_1(\pi\pi^*)$, $T_N(n_N\pi^*)$, and $T_1(\pi\pi^*)$ hypersurfaces, shapes of the HOMO and LUMO natural orbitals, and complete ref 39. This material is available free of charge via the Internet at http://pubs.acs.org.

References and Notes

(1) Voet, D.; Voet, J. *Biochemistry*; John Wiley and Sons, Inc.: New York, 1990.

(2) Briggs, W. R.; Beck, C. F.; Cashmore, A. R.; Christie, J. M.; Hughes, J.; Jarillo, J. A.; Kagawa, T.;. Kanegae, H.; Liscum, E.; Nagatanni, A.; Okada, K.; Salomon, M.; Rüdiger, R.; Sakai, T.;. Zakano, M.; Wada, M.; Watson, J. C. *Plant Cell* **2001**, *13*, 993.

(3) Dürr, H.; Bouas-Laurent, H. *Photochromism Molecules and Systems*; Elsevier Science: New York, 2003.

(4) Christie, J. M.; Salomon, M.; Nozue, K.; Wada, M.; Briggs, W. R. *Proc. Natl. Acad. Sci. U.S.A.* **1999**, *96*, 8779.

(5) Swartz, T. E.; Corchnoy, S. B.; Christie, J. M.; Lewis, J. W.; Szundi, I.; Briggs, W. R.;. Bogomolni, R. A. *J. Biol. Chem.* **2001**, *276*, 36493.

(6) Neiss, C.; Saalfrank, P. *Photochem. Photobiol.* **2003**, *77*, 101.

(7) Kennis, J. T. M.; Crosson, S.; Gauden, M.; Stokkum, I. H. M.; Moffat, K.; van Grondelle, R. *Biochemistry* **2003**, *42*, 3385.

(8) Kottke, T.; Heberle, J.; Hehn, D.; Dick, B.; Hegemann, P. *Biophys. J.* **2003**, *84*, 1192.

(9) Scheleicher, E.; Kowalczyk, R. M.; Kay, C. W. M.; Hegemann, P.; Bacher, A.; Fischer, M.; Bittl, R.; Richter, G.; Weber, S. *J. Am. Chem. Soc.* **2004**, *126*, 11067.

(10) Crovetto, L.; Braslavsky, E. *J. Phys. Chem. A* **2006**, *110*, 7307 and references cited therein.

(11) Kowalczyk, R. M.; Schleicher, E.; Bittl, R.; Weber, S. *J. Am. Chem. Soc.* **2004**, *126*, 11393.

(12) Song, P.-S. *J. Phys. Chem.* **1968**, *72*, 536.

(13) Wouters, J.; Durant, F.; Champagne, R.; André, J. M. *Int. J. Quantum Chem.* **1997**, *64*, 721.

(14) Sikorska, E.; Khmelinskii, I. V.; Koput, J.; Bourdelande, J. L.; Sikorski, M. *J. Mol. Struct.* **2004**, *697*, 137.

(15) Sun, M.; Moore, T. A.; Song, P.-S. *J. Am. Chem. Soc.* **1972**, *94*, 5.

(16) Johansson, L. B.-A.; Davidsson, A.; Lindblom, G.; Naqvi, K. R. *Biochemistry* **1979**, *18*, 4249.

(17) Andersson, K.; Malmqvist, P.-Å.; Roos, B. O. *J. Chem. Phys.* **1992**, *96*, 1218.

(18) Roos, B. O.; Fülscher, M. P; Malmqvist, P.-Å.; Merchán, M.; Serrano-Andrés, L. *Theoretical Studies of Electronic Spectra of Organic Molecules*; Langhoff, S. R., Ed.; Kluwer Academic Publishers: Dordrecht, The Netherlands, 1995; p 357.

(19) Roos, B. O.; Andersson, K.; Fülscher, M. P.; Malmqvist, P.-Å.; Serrano-Andrés, L.; Pierloot, K.; Merchán, M. *Adv. Chem. Phys.* **1996**, *93*, 219.

(20) Merchán, M.; Serrano-Andrés, L.; Fülscher, M. P.; Roos, B. O. *Multiconfigurational Perturbation Theory Applied to Excited States of Organic Compounds*; Hirao, K., Ed.; World Scientific Publishing Company: Amsterdam, 1999; Vol. 4, p 161.

(21) Merchán, M.; Serrano-Andrés, L. In *Computational Chemistry*; Olivucci, M., Ed; Elsevier: Amsterdam, 2005.

(22) Serrano-Andrés, L.; Merchán, M. In *Encyclopedia of Computational Chemistry*; Schleyer, P. v. R., Schreiner, P. R., Schaefer, H. F., III, Jorgensen, W. L., Thiel, W., Glen, R. C., Eds.; Wiley: Chichester, U.K. 2004.

(23) (a) Serrano-Andrés, L.; Merchán, M.; Nebot-Gil, I.; Roos, B. O.; Fülscher, M. *J. Am. Chem. Soc.* **1993**, *115*, 6184. (b) Roos, B. O.; Malmqvist, P.-Å.; Molina, V.; Serrano-Andrés, L.; Merchán, M. *J. Chem. Phys.* **2002**, *116*, 7526. (c) Serrano-Andrés, L.; Fülscher, M. P.; Roos, B. O.; Merchán, M. *J. Chem. Phys.* **1996**, *100*, 6484.

(24) (a) Merchán, M.; Roos, B. O. *Theor. Chim. Acta* **1995**, *92*, 227. (b) Merchán, M.; Roos, B. O.; McDiarmid, R.; Xing, X. *J. Chem. Phys.* **1996**, *104*, 1791.

(25) (a) Pou-Amérigo, R.; Merchán, M.; Ortí, E. *J. Chem. Phys.* **1999**, *110*, 9536. (b) Pou-Amérigo, R.; Serrano-Andrés, L.; Merchán, M.; Ortí, E.; Forsberg, N. *J. Am. Chem. Soc.* **2000**, *122*, 6067.

(26) Climent, T.; González-Luque, R.; Merchán, M. *J. Phys. Chem. A* **2003**, *107*, 6995.

(27) González-Luque, R.; Garavelli, M.; Bernardi, F.; Merchán, M.; Robb, M. A.; Olivucci, M. *Proc. Natl. Acad. Sci. U.S.A.* **2000**, *97*, 9379.

(28) Molina, V.; Merchán, M. *Proc. Natl. Acad. Sci. U.S.A.* **2001**, *98*, 4299.

(29) Merchán M.; Serrano-Andrés, L. *J. Am. Chem. Soc.* **2003**, *125*, 8108.

(30) Serrano-Andrés, L.; Merchán, M.; Borin, A. C. *Proc. Natl. Acad. Sci. U.S.A.* **2006**, *103*, 8691.

(31) For reviews of the CASSCF methods, see different contributions in: *Ab Initio Methods in Quantum Chemistry—II*; Lawley, K. P., Ed.; Wiley: New York, 1987.

(32) Forsberg, N.; Malmqvist, P.-Å. *Chem. Phys. Lett.* **1997**, *274*, 196.

(33) Malmqvist, P.-Å. *Int. J. Quantum Chem.* **1986**, *30*, 479.

(34) Malmqvist, P.-Å.; Roos, B. O. *Chem. Phys. Lett.* **1989**, *155*, 189.

(35) Strickler, S. J.; Berg, R. A. *J. Chem. Phys.* **1962**, *37*, 814.

(36) Rubio-Pons, O.; Serrano-Andrés, L.; Merchán, M. *J. Phys. Chem. A* **2001**, *105*, 9664.

(37) De Vico, L.; Olivucci, M.; Lindh, R. *J. Chem. Theory Comput.* **2005**, *1*, 1029.

(38) Merchán, M.; Serrano-Andrés, L.; Robb, M. A.; Blancafort, L. *J. Am. Chem. Soc.* **2005**, *127*, 1820.

(39) Andersson, K.; et al. *MOLCAS*, version 6.0; Department of Theoretical Chemistry, Chemical Centre, University of Lund: Lund, Sweden, 2004.

(40) Veryazov, V.; Widmark, P.-O.; Serrano-Andrés, L.; Lindh, R.; Roos, B. O. *Int. J. Quantum. Chem.* **2004**, *100*, 626.

(41) Wang, M.; Fritchie, J., Jr. *Acta Crystallogr.* **1973**, *B29*, 2040.

(42) Visser, A. J. W. G.; Müller, F. *Helv. Chim. Acta* **1979**, *62*, 593.

(43) Serrano-Andrés, L.; Forsberg, N.; Malmqvist, P.-Å. *J. Chem. Phys.* **1998**, *108*, 7202.

(44) Eaton, W. A.; Hofrichter, J.; McKinen, M. W.; Andersen, D. R.; Ludwig, M. L. *Biochemistry* **1975**, *14*, 2146.

(45) Turro, N. J. *Modern Molecular Photochemistry*; University Science Books: Sausalito, CA, 1991.

(46) Shüttrigkeit, T. A.; Kompa, C. K.; Salomon, M.; Rüdiger, W.; Michel-Beyerle, M. E. *Chem. Phys.* **2003**, *294*, 501.